

Computer Reconstruction of the Cardiac Pacemaker

OV Aslanidi, MR Boyett, H Zhang

University of Manchester, Manchester, UK

Abstract

Sinoatrial (SA) node, the pacemaker of the heart, is a structurally and functionally complex tissue. The role of this complexity in initiation and conduction of the pacemaker activity is not fully understood. Computer modeling provides a powerful alternative way to experiment in studying complex cardiac phenomena. In this work we combine histological, immunochemical, electrophysiological data with mathematical and computational approaches to reconstruct the first anatomically and biophysically detailed model of the rabbit SA node and the surrounding atrium. The model provides an efficient computational platform for studying complex functions of the cardiac pacemaker.

1. Introduction

Rhythmic beating of the heart is initiated by the cardiac pacemaker, the sinoatrial (SA) node. More than any other part of the heart the SA node is a complex tissue which function depends on its complexity [1]. The SA node is a heterogeneous tissue with substantial regional differences in cellular electrical properties, such as the cell membrane capacitance, ionic current densities and intercellular gap junction conductances. Gradients of these properties from the center to the periphery are believed to be essential for the SA node to drive, but not be suppressed by, the surrounding mass of atrial muscle [1-3]. However, knowledge of the role of complex tissue organization in the mechanisms of pacemaking is far from comprehensive, and is often limited by the lack of data for same species. The aim of this work is to construct a unified, anatomically and biophysically detailed computer model of the cardiac pacemaker comprising the rabbit SA node and the surrounding atrium.

2. Methods

Dynamics of electrical variables in cardiac tissues can be described by the Hodgkin-Huxley-type nonlinear partial differential equation (PDE) [4]:

$$\frac{\partial V}{\partial t} = \nabla(\mathbf{D}\nabla V) - C_m^{-1}I_{ion} \quad (1)$$

Here V (mV) the membrane potential, ∇ a spatial gradient operator defined within the tissue geometry, t time (s). \mathbf{D} is the effective diffusion tensor ($\text{mm}^2 \text{ms}^{-1}$) that characterizes cell-to-cell spread of voltage via gap junctions. C_m (pF) is the cell membrane capacitance, I_{ion} the total membrane ionic current density (pA). Various biophysically detailed mathematical models have been developed to describe the voltage and time dependent current I_{ion} , and hence, action potential (AP) properties – primarily in the rabbit (species for which most data are available) SA node [5], as well as atrial cells [6].

2.1. Biophysical models

We use the model of Zhang et al. [5], which generates APs similar to those recorded experimentally for the center (leading pacemaker site) and the periphery (exit pathway) of the rabbit SA node. The model introduces a gradient of cellular electrical properties, primarily the cell membrane capacitance C_m , which changes from 20 pF in the center to 65 pF at the periphery. The membrane ionic current densities are correlated with C_m , as reported experimentally. The resultant model reproduces regional differences in AP properties within the SA node (Fig. 1).

A similar gradient in the cell-to-cell coupling, which increases substantially from the center to periphery of the SA node, is introduced to account for the experimental observations [7, 8]. Three-dimensional analytical expressions for both gradients are as follows:

$$\begin{aligned} C_m(x, y, z) &= 20 + \sqrt{c_x^2 + c_z^2} (65 - 20) \\ c_x &= \frac{1}{1 + \exp[-0.1(x - 9.4)]} + \frac{1}{1 + \exp[0.1(x - 7.0)]} \\ c_z &= \frac{1}{1 + \exp[-0.04(z - 7.2)]} + \frac{1}{1 + \exp[0.04(z - 2.4)]} \end{aligned} \quad (2)$$

$$\begin{aligned} G(x, y, z) &= 0.01 + \sqrt{g_x^2 + g_z^2} (1 - 0.01) \\ g_x &= \frac{1}{1 + \exp[-0.5(x - 9)]} + \frac{1}{1 + \exp[0.5(x - 7.4)]} \\ g_z &= \frac{1}{1 + \exp[-0.2(z - 6.4)]} + \frac{1}{1 + \exp[0.2(z - 3.2)]} \end{aligned} \quad (3)$$

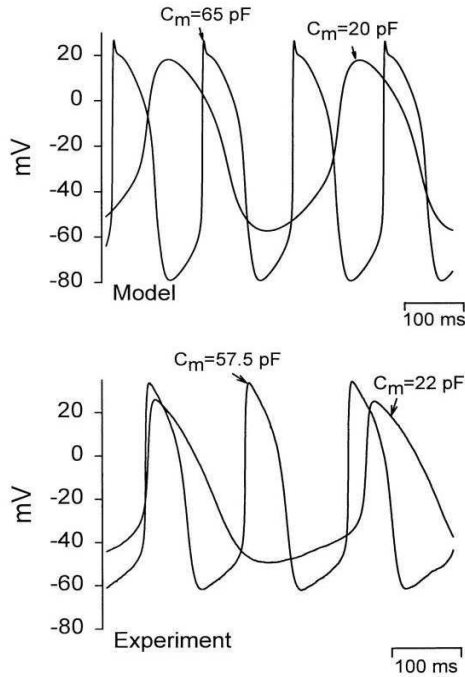


Figure 1. APs from the centre and the periphery of the rabbit SA node: model of Zhang et al. [5] (top), and the respective experimental recordings (bottom). From [5].

The ionic current of rabbit atrial cells is described by the model of Lindblad et al. [6]. We modify the model to incorporate experimentally observed differences in the AP properties between two primary atrial cell-types, the crista terminalis (CT) and pectinate muscle (PM) cells. The modifications include changes of several specific ionic currents comprising I_{ion} : faster inactivation of I_{Na} , a 200% increase of the density of I_{CaL} , 500% increase of the density of I_{K1} , and addition of a steady state component, $I_{sus} = g_{sus} (V - V_K)$, to I_{to} . Regional differences between CT and PM cells are introduced primarily as different current densities of I_{to} and I_{sus} : both currents are twice larger in PM cells than in CT cells (note that the density of I_{to} is decreased to 30% in CT and to 60% in PM in respect to the original model). These modifications are in agreement with experimental data [9], and APs generated with the model fit well to the experimental recordings (Fig. 2).

2.2. Anatomical models

Previous models of the SA node have used simplified tissue geometries, such as a one-dimensional stand [1] or a two-dimensional tissue slice [10]. None of the models accounted for anisotropy of the SA node and the atrial tissue. However, in cardiac tissues, cylindrical cells are aligned parallel to each other, and excitation is conducted more rapidly along fibres than across them [11]. The SA

node and the surrounding atrium, primarily, have a characteristic pattern of fibers orientated along the bundles of crista terminalis and atrial pectinate muscles.

Detailed three-dimensional anatomical structure of the rabbit SA node and the surrounding atrial tissue has been reconstructed recently based on a combination of histological, immunochemical and electrophysiological experiments from our Lab [7]. The geometry presents a high resolution ($40 \mu\text{m}$) regular Cartesian grid of $375 \times 45 \times 240$ points. For each point a flag variable identifies whether it belongs to one of the following cell-types: central/peripheral SA node cells, CT/PM atrial cells, unexcitable connective tissue or the block zone of nodal cells with low excitability (in our model I_{CaL} and I_{Na} in the block zone are completely suppressed).

We update the geometry with fibre orientations, which is measured histologically for each grid point at the epicardial and endocardial surfaces of the tissue (Fig. 3). As the tissue is very thin (less than 1 mm), and these two patterns are quite similar to each other, we assume that the fibre orientation does not change through the depth of the tissue. For same reasons the gradients C_m and G in our model do not change with the depth (along the y -axis). Values of diffusion coefficients along and across the fibres in our model are $D_{||} = 5 \text{ mm}^2 \text{ ms}^{-1}$ and $D_{\perp} = 0.5 \text{ mm}^2 \text{ ms}^{-1}$, respectively. Linear combinations of the fibre orientation vectors with these diffusion coefficients give

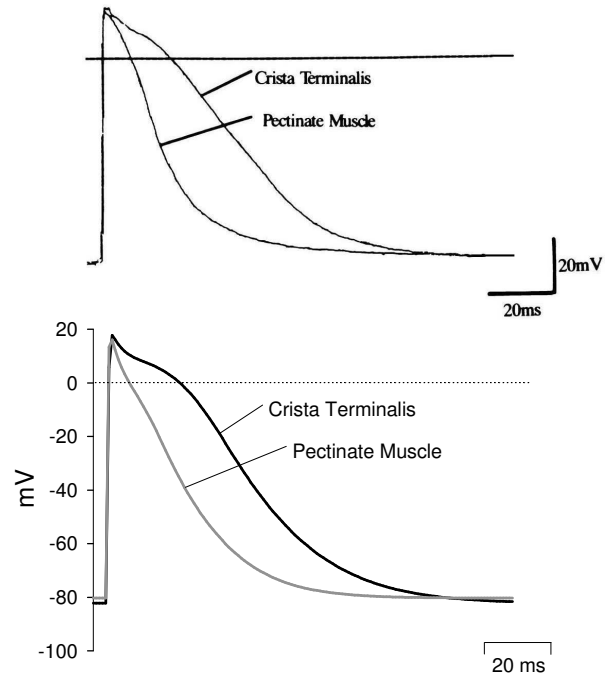


Figure 2. APs in two rabbit atrial cell-types: experimental recordings (top, from [9]), and simulations with the modified model of Lindblad et al. [6] (bottom).

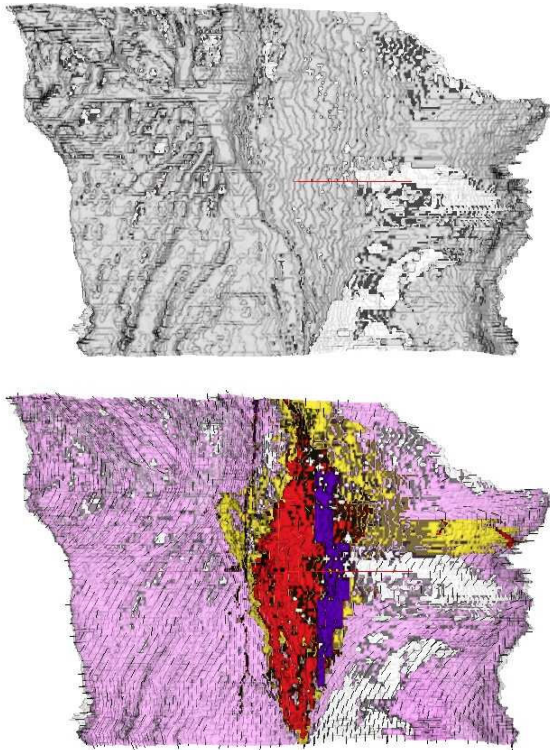


Figure 3. Reconstructed architecture of the rabbit SA node and the surrounding atrial tissue. Top: geometry comprising excitable (dark grey) and connective (light grey) tissues; CT is the thick bundle crossing the tissue vertically, smaller PMs branch to the left. Bottom: fibre orientations (black lines) and cell heterogeneity (red is the SA node centre, yellow is periphery, blue is the block zone, pink and light grey are atrial and connective tissues, respectively) within the semi-transparent geometry.

components of the diffusion tensor, \mathbf{D} , at each grid point [4]. Besides, at each grid point these components are further multiplied by the respective values of the dimensionless coupling gradient G , defined by eqn. (3).

The equation (1) is solved on the geometry grid using a finite-difference PDE solver that implements the explicit Euler method with time and space steps $\Delta t = 0.01$ ms and $\Delta x = 0.04$ mm, respectively. As solving a system of nonlinear partial differential equation on a ~4-million-point grid is a very computationally demanding task, our C-code implementing the PDE solver was parallelized under MPI and run on 96 SGI Origin 3000 CPUs of the CSAR supercomputer (Manchester, UK). Parallel fraction of the code was 95%, and simulating 1 second of the pacemaker activity took about 4 hours.

Thus, a high-resolution model incorporating detailed anatomy, cell variability, fibre orientations and electrical gradients within the rabbit pacemaker (comprising the SA

node and the surrounding atrial tissue) has been constructed and effectively implemented.

3. Results

Computer simulations with the reconstructed model reproduce essential features of the patterns of electrical activity in the rabbit pacemaker, observed in experiments [1]. Subsequent snapshots of an excitation wave spreading through the pacemaker are shown in Fig. 4 for the moments of time $t = 20, 80, 110$ and 170 ms. First, an action potential is generated spontaneously from uniform initial conditions ($V = -80$ mV in all cells) in the centre of the SA node; although the central nodal cells have lower intrinsic oscillation frequency (see Fig. 1), they overtake the faster peripheral cells that are suppressed by the load of more hyperpolarized atrium (the reversal potential is about -80 mV at the SA node periphery, and -85 mV in the atrial cells). This AP initiates an excitation wave slowly propagating from the SA node center to the periphery, towards CT and the left atrium. Propagation in the opposite direction, towards the atrial septum, is prevented by the block zone. When excitation reaches the atrial tissue, it rapidly propagates through the fibres orientated along the crista terminalis, and then evades rest of the left atrium through the bundles of pectinate muscles. Finally, when the whole left atrium is excited, the wave travels around the block zone and spreads into the atrial septum, towards the right atrium. This cycle is repeated over and over with the period of about 300 ms. Thus, simulated electrical activation sequence, the overall wave pattern, the wave propagation velocity and the pacemaker oscillations frequency are consistent with the experimental data [1].

4. Discussion and conclusions

Our computer reconstruction of the cardiac pacemaker captures the most essential features of the structure and function of the rabbit SA node. Combining detailed cell excitation models with the tissue geometry and fibre orientations allows simulations of the complex patterns of electric activity within the pacemaker. Importantly, the imposed gradients of cell electrical properties not only account for variability of the AP shape, duration and intrinsic oscillation rate, but are also responsible for the correct activation sequence in the tissue: the SA node center is excited first, then the periphery, the left atrium, and finally the right atrium. Without the gradients in the membrane capacitance and the cell-to-cell coupling, peripheral nodal cells would overtake the intrinsically slower central cells, violating the activation sequence. The gradient in cell-to-cell coupling also act as a coupling

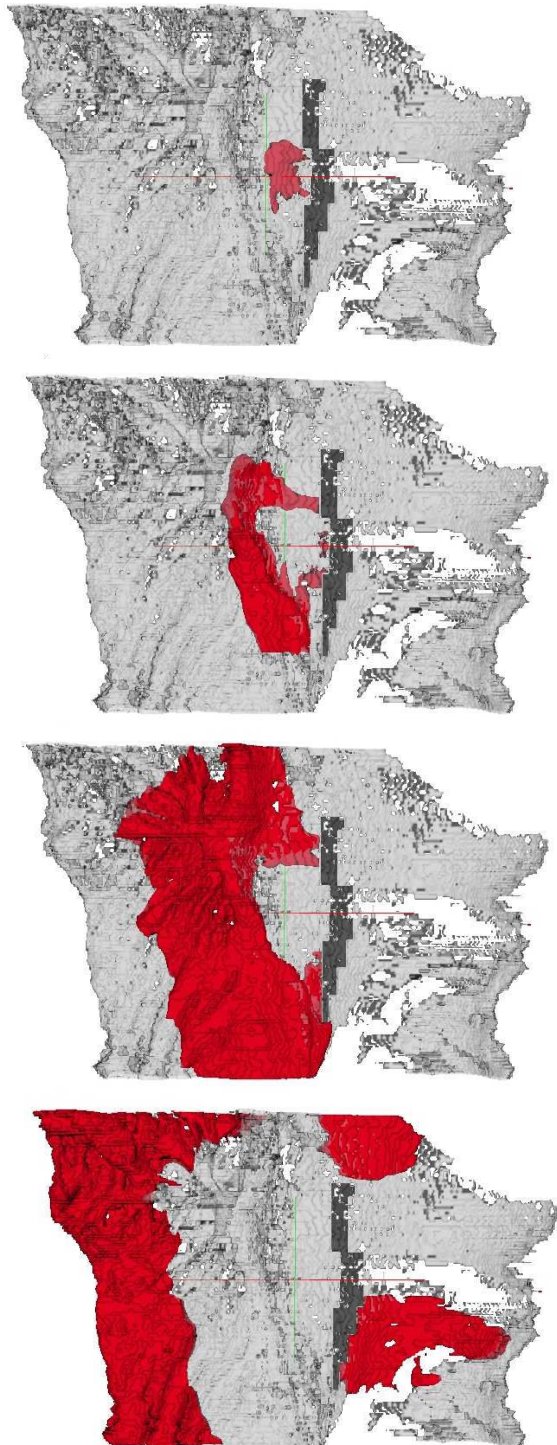


Figure 4. Patterns of electrical activity in the cardiac pacemaker model. Isosurfaces of the membrane potential at $V = -30$ mV demonstrate four subsequent positions of an excitation wave (top to bottom): initial generation of the wave in the SA node center, its exit from the periphery into CT, rapid propagation along the PM bundles, and spread around the block zone (dark grey area). Red and green lines are x and z axis, respectively.

barrier preventing total suppression of the SA node by electrotonic currents from more hyperpolarized atrium.

In summary, we have reconstructed an anatomically and biophysically detailed computer model, which reproduces complex spatiotemporal patterns of electrical activity in the rabbit SA node and the surrounding atrium, and can provide insights into the mechanisms of wave generation and conduction during pacemaking.

Acknowledgements

This research was funded by the BBSRC (UK).

References

- [1] Boyett MR, Honjo H, Kodama I. The sinoatrial node, a heterogeneous pacemaker structure. *Cardiovasc Res* 2000; 47:658-87.
- [2] Joyner RW, van Capelle FJ. Propagation through electrically coupled cells. How a small SA node drives a large atrium. *Biophys J* 1986; 50:1157-64.
- [3] Kirchhof CJ, Bonke FI, Allessie MA et al. The influence of the atrial myocardium on impulse formation in the rabbit sinus node. *Pflügers Arch* 1987; 410:198-203.
- [4] Fenton FH, Karma A. Vortex dynamics in three-dimensional continuous myocardium with fibre rotation: Filament instability and fibrillation. *Chaos* 1998; 8:20-47.
- [5] Zhang H, Holden AV, Kodama I et al. Mathematical models of action potentials in the periphery and center of the rabbit sinoatrial node. *Am J Physiol Heart Circ Physiol* 2000; 279:H397-421.
- [6] Lindblad DS, Murphey CR, Clark JW et al. A model of the action potential and underlying membrane currents in a rabbit atrial cell. *Am J Physiol* 1996; 271:H1666-96.
- [7] Sano T, Yamagishi S. Spread of excitation from the sinus node. *Circ Res* 1965; 16:423-30.
- [8] Dobrzynski H, Li J, Tellez J et al. Computer three-dimensional reconstruction of the sinoatrial node. *Circulation* 2005; 111:846-54.
- [9] Yamashita T, Nakajima T, Hazama H et al. Regional differences in transient outward current density and inhomogeneities of repolarization in rabbit right atrium. *Circulation* 1995; 92:3061-9.
- [10] Garny A, Noble D, Kohl P. Dimensionality in cardiac modelling. *Prog Biophys Mol Biol* 2005; 87:47-66.
- [11] Nielson PMF, LeGrice IJ, Smaill BH et al. Mathematical model of the geometry and fibrous structure of the heart. *Am J Physiol Heart Circ Physiol* 1991; 260:H1365-78.

Address for correspondence

Oleg Aslanidi, Ph.D.

School of Physics and Astronomy
The University of Manchester
Manchester M13 9PL
United Kingdom